Second-Harmonic Contactless Method for Measurement of RMS Current Using a Standard Infrared Camera

Błażej Torzyk and Bogusław Więcek

Abstract— **This article presents a new method for measuring rms values of alternative current (ac) in power lines using an infrared (IR) camera. An IR camera registers thermal images in time with an appropriate frame rate in order to calculate the spectrum of the temperature signal of a power cable. For the European standard, the amplitudes of the harmonics for $f \approx 100$ Hz correlate to the power dissipated in a conductor. The fast Fourier transform (FFT) and rms analysis for different current values were performed. The obtained results allow plotting the calibration curve of temperature changes versus the rms values of the current flowing in wire. They confirmed the linear relation between the 100-Hz spectral component of the temperature and the square value of the rms current. This method has unique advantages. It is noncontact and makes it possible to estimate the rms current regardless of the ambient background radiation and convection cooling conditions having a significant impact on overhead lines, in particular.**

Index Terms— **Current measurement, electric variables measurement, harmonic analysis, infrared (IR) imaging, power transmission, thermal analysis.**

I. INTRODUCTION

THE growing demand for energy requires the continuous monitoring of power systems and measuring current, voltage, temperature, and power using effective contact and contactless methods [1]. At present, low-cost current transformers are typically used for current measurement [10]–[12]. The evaluation of ac current by such elements uses the magnetic field generated by the current flow in a conductor. As a consequence, the voltage over the winding at the ferromagnetic core is inducted and used to measure the value of the rms current. Monitoring power lines in this way has some disadvantages. First of all, it is a kind of proximity measurement, where the distance between the line and the sensor is relatively small. In consequence, it does not allow measuring from a distance which is safe for an operator. Moreover, such monitoring is only available for cables and lines which are easy to access. In practice, it is impossible to use transformers to monitor current, e.g., along overhead lines.

In order to increase the safety of power delivery, infrared (IR) systems can be applied, in particular in the case

of open-air power grid monitoring [2], [3]. Sometimes airplanes/helicopters or unmanned aerial vehicles (UAVs) equipped with high-resolution IR cameras are used [13]. Besides power transformer and IR systems, fiber optical sensors are used today as well. They exist as distributive temperature sensing (DTS) allowing measurements of temperature along a distance of a few kilometers with the resolution of about 1 m and accuracy of 1 °C [14]. An additional advantage of optical fibers is that they are indifferent to an electromagnetic field and allow measuring temperatures in real time.

The methods mentioned above are implemented in various industrial and everyday life applications. For example, such temperature monitoring is recommended for landfill sites, fire alarm systems, optimization of heat losses in buildings, and stresses in constructions or in server rooms.

The aim of this research was to develop a new method for measuring alternating current using an IR camera. Applications of the aforementioned methods ensuring security in energy delivery allow contactless measurement of temperature and flowing current at any point. The accuracy of the obtained results depends on the quality of the IR camera used [2]. The test consists of registering temperature changes in a varnished steel wire using an IR camera for various current values flowing through a conductor. The subsequent analysis and processing of the temperature signal versus time make it possible to estimate the rms value of the current. The data is subjected to frequency analysis in order to obtain the spectrum of harmonics of the tested signal [7], [18]. Using the algorithm elaborated in this research allows determining the dependence of current and temperature changes [8], [9]. All considerations presented in the article refer to European power standard and can be easily extended to the 60 Hz network.

II. CONCEPT OF MEASUREMENT OF AC CURRENT RMS VALUE

In the general case, the typical current in electrical wire is not sinusoidal, especially in low-voltage electrical systems. It is due to the impulse power conversion used in low-voltage systems to control power effectively. Although, the power factor correction (PFC) is obligatory today, there are still some higher frequency components in a current consumed from the power system [7], [18]. Nonsinusoidal current can be represented using the Fourier series, typically with odd spectral components (1). The odd current's harmonics are

only generated if electrical current is switched ON and OFF identically for both half-periods of the sinusoidal signal. It is the typical scenario of power control in low-voltage electrical network [18]

$$I(t) = I_{50}\cos(\omega_{50}t) + I_{150}\cos(\omega_{150}t + \varphi_{150}) + \cdots \quad (1)$$

where I_{50}, I_{150}, ω_{50}, and ω_{150} denote amplitudes and angular frequencies of the fundamental and third-order harmonic of current, respectively and φ_{150} is the phase shift for third-order harmonic.

Due to the requirements of using PFC in new electrical systems, the higher harmonics contents are decreasing. In this research, we assume that the current is described as

$$I \approx I_{50}\cos(\omega_{50}t). \quad (2)$$

In consequence, power dissipated in a cable takes the forms

$$P(t) = I_{50}^2 R_{\text{cable}} \frac{1 + \cos(2\omega_{50}t)}{2} \quad (3)$$

$$P(t) = P_{\text{mean}} + P_{100}\cos(\omega_{100}t). \quad (4)$$

The power dissipated in a cable consists of two equal parts: the mean and 100-Hz component values [1], [6], [7]. The main idea of the proposed new method is to correlate the temperature of a wire not with mean power but with the spectral component of current for a frequency of $f = 100$ Hz.

In order to evaluate the level of temperature in the ac domain for different frequencies of power excitation, the thermal impedance in frequency domain $Z_{\text{th}}(j\omega)$ has to be determined [6], [7], [19], [22]. Thus, temperature can easily be evaluated as

$$T(j\omega) = Z_{\text{th}}(j\omega)P(j\omega) \quad (5)$$

$$T_{\text{mean}} = R_{\text{th}}P_{\text{mean}} \quad (6)$$

$$T_{100} = Z_{\text{th}100}P_{100} \quad (7)$$

where $Z_{\text{th}100}$ is the modulus of thermal impedance for $f = 100$ Hz.

In the general case $P_{\text{mean}} = P_{100}$, where P_{100} is the amplitude of 100-Hz harmonic of the power excitation. Unfortunately, the modulus of $Z_{\text{th}100}$ is much lower than R_{th} ($Z_{\text{th}100} \ll R_{\text{th}}$). This results in very low temperature oscillations for $f = 100$ (Hz) ($T_{100} \ll T_{\text{mean}}$).

The amplitude of ac power P_{100} can be evaluated as

$$P_{100} = \frac{I_{50}^2 \rho_e l}{2S} \quad (8)$$

where ρ_e is the electrical resistivity of a cable and l and S denote the length and cross section area of a cable, respectively.

In summary, the proposed new method of current measurement in ac electrical power systems consists of the measurement of the 100-Hz spectral component of temperature caused by a 50-Hz electrical current flow in a cable [7]. That is the reason to use the term "second-harmonic" for the proposed new method of the temperature and rms current measurement.

For this purpose, the application of an IR thermal camera allowing contactless temperature measurement is proposed. One has to bear in mind that the newest IR systems allow
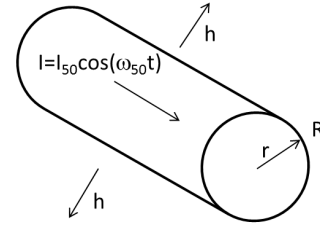

Fig. 1. Cable modeled as a metal cylinder conducting the current with the first harmonic component.

measuring the minimum temperature difference in the range of tens of millikelvin. The noise equivalent temperature difference (NETD) for cooled, photon IR thermal systems approaches 18 mK today [3]. Therefore, a simple analytical heat transfer model was elaborated to estimate the resolution of IR temperature measurements needed [1], [4]–[6], [19]–[22].

III. THERMAL MODEL OF AN ELECTRICAL CABLE IN AC DOMAIN

In order to elaborate and confirm the correctness of the new method of measuring the current in ac overhead line wire using IR cameras, first a simple thermal model of heat transfer in a cable was worked out. The wire is a metal (e.g., steel) cylinder with a radius R, as shown in Fig. 1. It is surrounded by air and the heat dissipated in it is transferred to ambient by free convection described by the heat transfer coefficient h. At this stage of the research, we assume the first-harmonic current I flowing through the cable only.

Heat transfer in solids is presented by the Fourier–Kirchhoff (1)

$$k\nabla^2 T(r) - C_v \frac{\partial T(r)}{\partial t} = -p_v \quad (9)$$

where k–thermal conductivity of the wire, C_v–volumetric thermal capacity($C_v = \rho \cdot c_s$, ρ–density, c_s–specific heat), and p_v–power density in (W/m^3) [16], [17].

By introducing the diffusion length L for the material the cable is made of, and converting the model into the ac domain using the Laplace transform (for $s = j\omega$), we can simplify the heat transfer (9) [1], [4], [5]

$$\nabla^2 T(r) - \frac{T(r)}{L^2} = -\frac{p_v}{k} \quad (10)$$

where diffusion length L is determined by the following equation:

$$L = \sqrt{\frac{k}{j\omega C_v}} \quad (11)$$

where $\omega = 2\pi f$ is the angular frequency.

The Laplace transform reduces the heat transfer equation by eliminating the temperature derivative in time (11). The additional simplification of a 2-D analytical thermal model of an electrical cable is achieved by taking advantage of cylindrical symmetry (11) [4], [6], [7]

$$\frac{\partial^2 T(r)}{\partial r^2} + \frac{1}{r}\frac{\partial T(r)}{\partial r} - \frac{T(r)}{L^2} = -\frac{p_v}{k}. \quad (12)$$
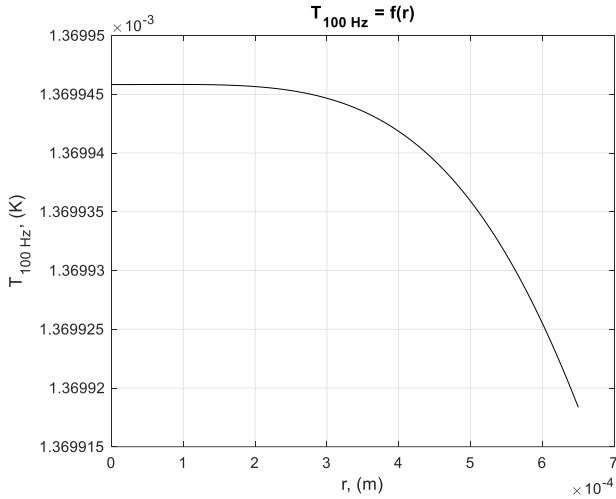
Fig. 2. Temperature distribution in the cable for $I_{rms} = 6.24$ A and $f = 100$ Hz.

Fig. 3. Amplitudes of temperature for different rms values of the current, $f = 100$ Hz.

Next the substitution $\rho = (r/L)$ allows getting the final form of the model which is known in heat transfer theory as the modified Bessel given by the following equation:

$$\frac{\partial^2 T(\rho)}{\partial \rho^2} + \frac{1}{\rho}\frac{\partial T(\rho)}{\partial \rho} - T(\rho) = -\frac{p_v}{j\omega C_v} \quad (13)$$

$$T(r) = AI_0\left(\frac{r}{L}\right) + \frac{p_v}{j\omega C_v} \quad (14)$$

where I_0 is the zero-order modified Bessel functions of the first kind.

The integration constant A can be derived from the boundary condition (15) for $r = R$, which assumes the removal of dissipated heat by convection to ambient

$$-k\frac{\partial T(r)}{\partial r}\bigg|_{r=R} = hT|_{r=R} \quad (15)$$

$$A = -\frac{h\frac{p_v}{j\omega C_v}}{\frac{k}{L}I_1\left(\frac{R}{L}\right) + hI_0\left(\frac{R}{L}\right)} \quad (16)$$

where I_1 is the first-order modified Bessel functions of the first kind and h is the heat transfer coefficient describing the free convection, and R is the radius of the wire.

The proposed model allows the calculation of temperature distribution in a wire for different values of frequency of power excitation. A few simulations were performed for a wire made of steel, with $2R = 1.3$ mm diameter, electrical resistivity $\rho_e = 0.15 \cdot 10^{-6}\,\Omega$m, thermal conductivity $k = 70$ W/mK, and thermal volumetric capacity $C_v = \rho \cdot c_s = 3\,851\,400$ J/m³K. The rms value of the heating current was varying in the range of 3–10 A and the cable was uniformly cooled by free convection with $h = 8$ W/m²K [16], [17].

As one can see in Fig. 2, the temperature of the cable is about of the order of magnitude of 1 mK for $I_{rms} = 6.24$ A of the flowing current, and frequency of the excitation power was $f = 100$ Hz. As expected, temperature is almost uniformly distributed inside the metal wire.

Furthermore, as expected, the amplitudes of temperature for the wire for $f = 100$ Hz are proportional to the square of the rms value of the flowing current, as shown in Fig. 3. In addition, we confirmed the very low value of the modulus
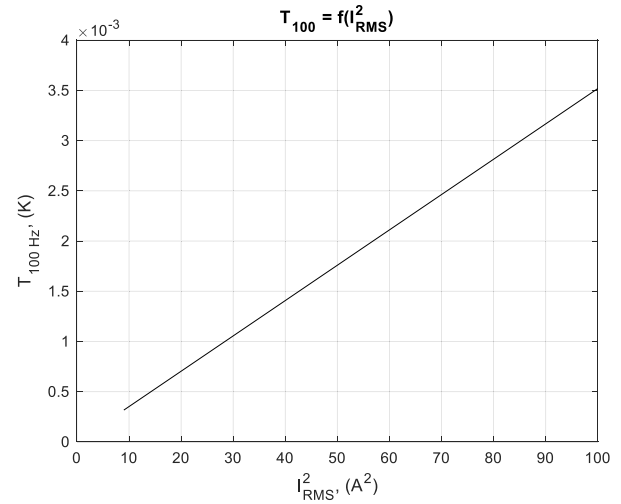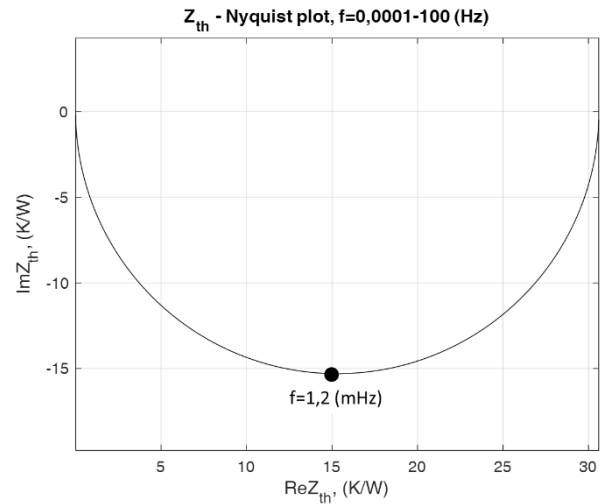

Fig. 4. Nyquist plot for a steel cable of 1 m length, 1.3 mm diameter, and cooled by free convection with $h = 8$ W/m²K, in the frequency range 0.001–100 Hz.

of thermal impedance for $f = 100$ Hz and, in consequence, the very low value of the measured temperature, far below the NETD limit of the best thermal cameras available today.

The Nyquist plot of the thermal impedance obtained from the simulations presented in Fig. 4 shows the values of thermal impedance Z_{th} for the cable used in the experimental part of this research. It approaches the value of zero for a frequency above a few hertz. In consequence, it makes it difficult to measure the very low temperature variation for $f = 100$ Hz.

The delay angle between temperature and power is almost $-90°$ for $f = 100$ Hz which denotes, that the considered dynamic thermal system has the capacitive character. In consequence, the temperature spectral component at frequency $f = 100$ Hz does not depend on resistive elements of the thermal model of a cable, i.e., on heat conduction in the cable and convection cooling at its edge. On the other hand, temperature variation depends very much on the thermal capacity and diameter of the cable and therefore, the proposed method needs calibration.
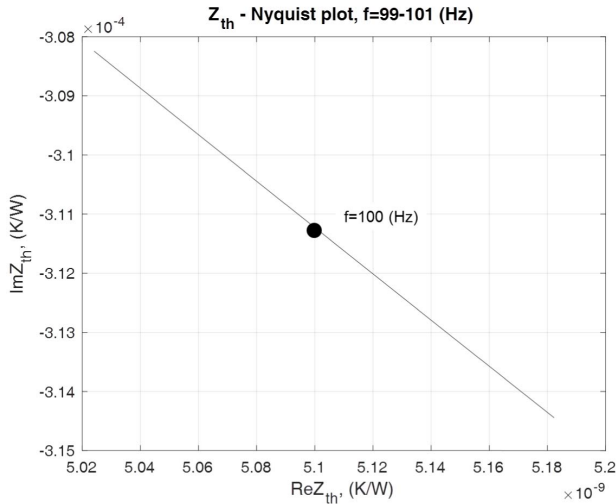
Fig. 5.   Nyquist plot for a steel cable of 1 m length, 1.3 mm diameter, and cooled by free convection with $h = 8$ W/m^{2}K, in the frequency range of 99–101 Hz.

TABLE I

AMPLITUDE OF TEMPERATURE SPECTRAL COMPONENT AND FOR DIFFERENT PARAMETERS OF THE WIRE, $f = 100$ Hz

Values of parameters in thermal modelling	Amplitude of the temperature component for f = 100 Hz
k = 70 (W/m·K), h = 8 (W/m^{2}K) C_v = 3851400 (J/m^{3}K), $2R$ = 0.0013 (m)	1.36991 (mK)
k = 400 (W/m·K), h = 100 (W/m^{2}K) C_v = 3851400 (J/m^{3}K), $2R$ = 0.0013 (m)	1.36988 (mK)
k = 70 (W/m·K), h = 8 (W/m^{2}K) C_v = 3851400 (J/m^{3}K), $2R$ = 0.002 (m)	0.24454 (mK)
k = 70 (W/m·K), h = 8 (W/m^{2}K) C_v = 3426500 (J/m^{3}K), $2R$ = 0.0013 (m)	1.53979 (mK)

Fig. 5 illustrates an interesting conclusion of heat transfer in solids. For high frequency (in this case for $f = 100$ Hz), the thermal mass behaves as a pure thermal capacity. As one can notice, $Z_{th} \approx (5.1 \cdot 10^{-9} - j3.11 \cdot 10^{-4})$ (K/W) $\approx 3.11/(j \cdot 10^4)$ (K/W). It can lead to thermal capacity equal to $C_{th} \approx 5.11$ J/K.

This fact has a significant impact on the results presented in Table I. The temperature amplitude for $f = 100$ Hz is independent of the heat transfer coefficient, i.e., from the convective cooling. It has the real practical meaning, especially for outdoor thermographic measurements of temperature and rms current.

The important advantage of the proposed method of temperature and current measurement in the ac domain is its independence from the heat transfer coefficient (cooling conditions), ambient temperature, and background radiation. These parameters are constant or vary very slowly and do not interfere with 100-Hz spectral component of temperature.

IV. MEASUREMENT SETUP

The measurements involving the registration of temperature changes in the electrical cable with a desired current require
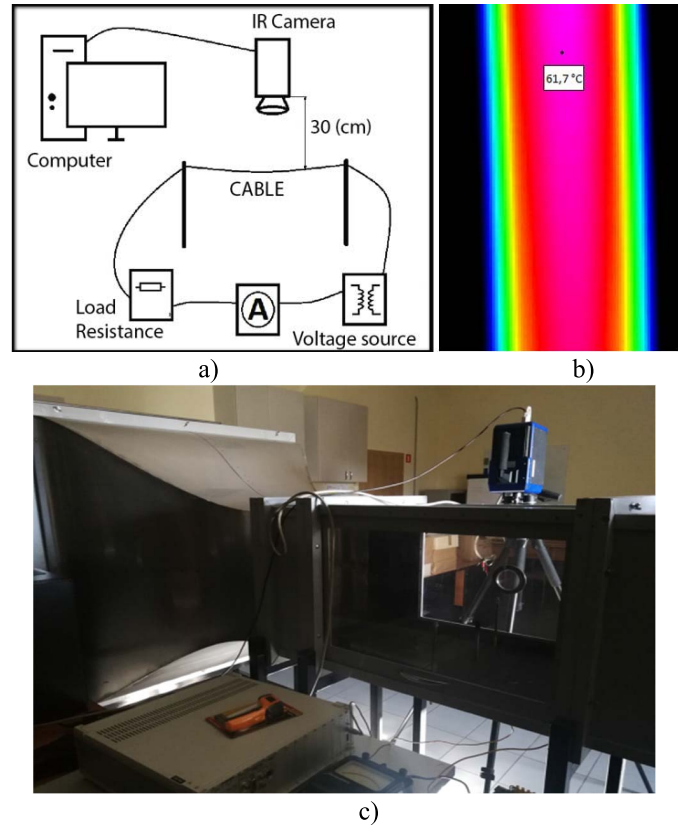

Fig. 6.   (a) Schematic layout, (b) with an example of the thermal image of the cable during heating, and (c) photograph in of the laboratory setup in the wind tunnel.

the construction of an appropriate laboratory stand (Fig. 6). The tested element is a simple model of a power line. It consists of a steel wire covered entirely with a thin layer of matte paint for equalizing and enraging emissivity. In practice, the emissivity depends mainly on the surface roughness. The power lines are not polished, and they are originally matte, which results in high value of emissivity. The problem of uneven emissivity distribution along the wire can be solved by measuring the maximum temperature in a chosen area of interest in thermal images.

The current flowing through the wire is forced by an additional load, which is changed to obtain the different current values. The system is powered by an additional safety extra low voltage (SELV) transformer, which, by filtering noise from the network, allows obtaining the required values of current at 24 VAC. The circuit is also equipped with an ac current meter that allows continuous monitoring of the lowest changes in the current value. Other necessary elements are a photon high-sensitive IR camera which is located centrally over the tested steel wire and computer tools to record temperature changes and then save them in the computer memory using dedicated software. In order to reduce and stabilize the heat losses to ambient, the wire was placed inside a low-speed wind tunnel. The wire was stretched on two vertical fasteners a few centimeter above floor level.

A high-speed middle wavelength IR (MWIR) photon thermal camera was used in the experiments–the Cedip–Titanium model equipped with 640×512 InSb cooled detector. The

thermal resolution NETD <18 mK allows registering thermal images of a reduced size with about 4 kHz frame rate. In this research thermal images were registered with $f_s = 870$-Hz sampling frequency. That is eight times more than the spectrum of the analyzed signals.

The camera was equipped with 50-mm lens. It allowed to get FOV = 11°. The pitch of the IR focal plane array (FPA) was 15 μm and in consequence instantaneous field of view (IFOV) was about 0.3 mrad. At a distance of 0.3 m from the camera, the minimum size of the object is about 0.18 mm. It was enough to measure temperature on the surface of the 1-mm diameter wire.

The duration of the recorded signal was 30 s, which gives 26 100 samples. In the beginning, the experiment was performed in a total lack of natural and artificial light. This sequence of measurements was performed 16 times for each of the three current values considered–5.4, 6.24, and 7.02 A. In order to check the impact of the radiation coming from the ambient, 30-s measurements were carried out in the presence of internal and external natural light.

Registered thermal images with a total number of samples equal to $N = 16 \cdot 26\,100 = 417\,600$ allowed determination of the measurement uncertainty [2]. Type-A uncertainty results from 16 repeated and averaged measurements of temperature given by the following equation:

$$u_A = \sqrt{\frac{\sum_{k=1}^{n} \left(T_{krms100} - \overline{T_{krms100}}\right)^2}{n(n-1)}} \approx 35.8 \cdot 10^{-6} (\text{K}). \quad (17)$$

Type-B uncertainty depends on NETD of an IR camera. Assume that the noise of the camera has at Gaussian distribution and it can be decreased by averaging with the factor $N^{0.5}$ the following equation:

$$u_B = \frac{\text{NETD}}{\sqrt{N}} \approx 28 \cdot 10^{-6} (\text{K}). \quad (18)$$

Finally, the extended uncertainty U_T for $n = 16$ averaged measurements with coverage factor $k = 2.12$ for 95% level of confidence id given by the following equation [2], [8]:

$$U_T = k\sqrt{u_A^2 + u_B^2} \approx 96.4 \cdot 10^{-6} (\text{K}). \quad (19)$$

V. RESULTS

A. Fast Fourier Transform (FFT) and RMS Analysis

The registered temperature signals versus time generated in the form of thermal images were analyzed using the FFT method. The region of interest containing the wire was selected manually and the average temperature versus time was calculated. Then, the FFT was run for the registered sequence of images to get 100-Hz component of the spectrum. The average values of 16 measuring sequences for each of three values of current were finally taken for the analysis. The results after FFT are presented in Table II and Figs. 7–9.

One can notice the level of noise mainly generated by the thermographic camera. Using the FFT and additional averaging, it is possible to reduce rms noise to the level lower than 100 μK.

TABLE II
MEAN VALUES OF TEMPERATURE OBTAINED USING FFT
ANALYSIS FOR $f = 100$ Hz

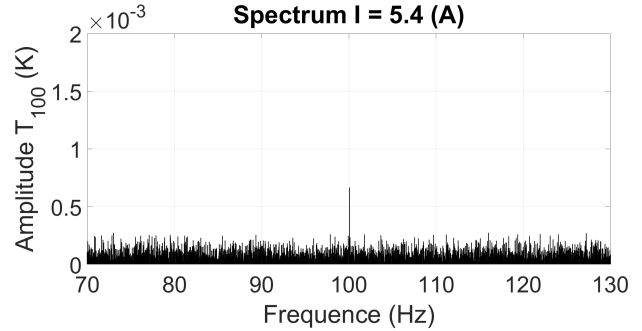| Current I (A)	5.4	6.24	7.02
Amplitude T_{100} (K)	$6.57 \cdot 10^{-4}$	$1.39 \cdot 10^{-3}$	$1.76 \cdot 10^{-3}$

Fig. 7. Temperature signal spectrum for 5.4 A rms current with dominating 100-Hz component.
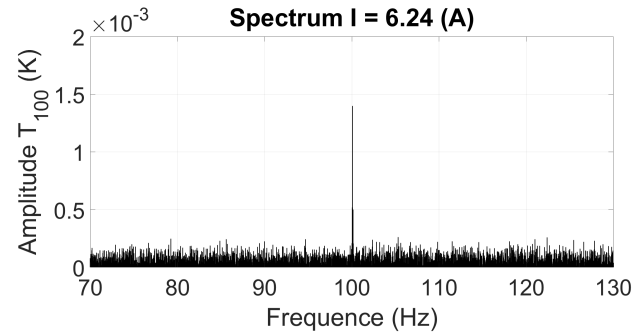

Fig. 8. Temperature signal spectrum for 6.24 A rms current with dominating 100-Hz component.
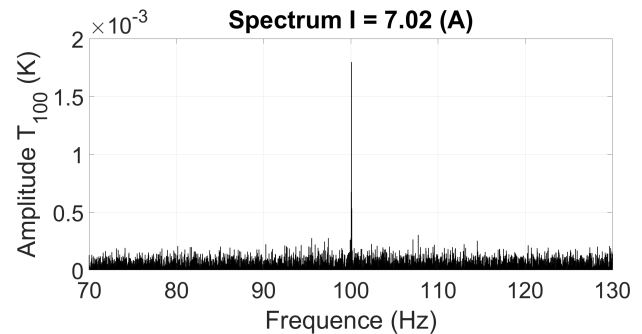

Fig. 9. Temperature signal spectrum for 7.02 A rms current with dominating 100-Hz component.

According to the theoretical assumptions and the results of modeling, the next step of this research was to determine the relationship between the rms current and the amplitude of the spectral component of temperature for $f \approx 100$ Hz. Two methods of evaluating the amplitude temperature of 100-Hz component of the spectrum were tested.

Using the first one, after FFT of temperature signal $T(t)$, the component with the maximum value in 97–103-Hz frequency range was taken for further analysis. This approach turned out not to be very accurate, mainly due to the leakage of the spectrum caused by unsynchronized (with camera image capturing) sampling of temperature.
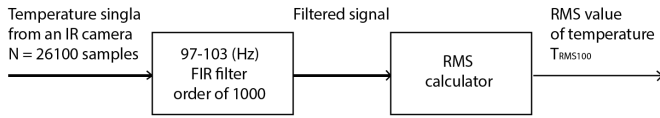
Fig. 10. Concept of calculating narrowband rms value of temperature.

Fig. 11. Linear relation between rms value of temperature in 97–103-Hz frequency range versus square of rms current.

The second method was based on calculating the rms value of temperature response $T_{\mathrm{rms}100}$ in a range next to central frequency $f = 100$ Hz. Experimentally, the region 97–103 Hz was chosen as sufficient to improve the accuracy. The linearity of the relation between the temperature for $f = 100$ Hz and the power dissipated (I_{rms}^2) in a cable was used as the criterion of accuracy. In order to select a narrow spectral band for the rms value of temperature calculation, a finite-impulse response (FIR) bandpass digital filter was used. After a few experimental trials, the order of the filter was 1000. The sequence of temperature samples $N = 26\,100$ was long enough to obtain a satisfactory result. The alternative method is to use FFT to get the rms value in the given frequency range. Such an approach was also tested, but, eventually, the FIR filtering was chosen as a faster method for further implementation in the prototype device.

Due to the leakage of the spectrum and the relatively significant level of noise, the estimate of 100 Hz component of the spectrum defined by the rms value of temperature ($T_{\mathrm{rms}100}$) correlated better with the rms current heating the wire. As expected, the estimate of narrowband rms for 100-Hz spectral component is proportional to the square of the rms current heating the wire, as shown in Fig. 11. Calculating the rms value of narrowband temperature signal for a frequency next to 100 Hz includes the surrounding noise. In consequence it overestimates the value of the 100-Hz spectral component of temperature. This effect can be noticed in Fig. 11 as the 300 μK offset of the presented characteristic. This offset can be reduced by additional averaging or by taking longer temperature sequences for filtering and analysis. It can also be arbitrarily eliminated as an impact of noise.

The proposed method for measuring the rms value of temperature in the range 97–103 Hz is presented in Fig. 10.

Table III presents the obtained rms values of temperature for the 97–103-Hz frequency range for different rms values of current flowing through a wire.

The results of the rms analysis show the linear nature of temperature changes versus the square of the rms current (power dissipated in a cable), as shown in Fig. 11, including the uncertainty intervals.

According the results in Table III, the range of temperature variation is 1.14–1.73 mK for rms values of current from 5.5 to 7.02 A. Fig. 11 is a kind of experimental calibration characteristic for the presented method. It has to be emphasized that such a calibration needs to be performed for any measured object.

Increasing the current and temperature in the wire can result in nonlinearity caused by temperature dependent resistivity. In the case of extended range of the measured current, temperature of 100-Hz spectral component will highly correlate with the rms current in the line as well.
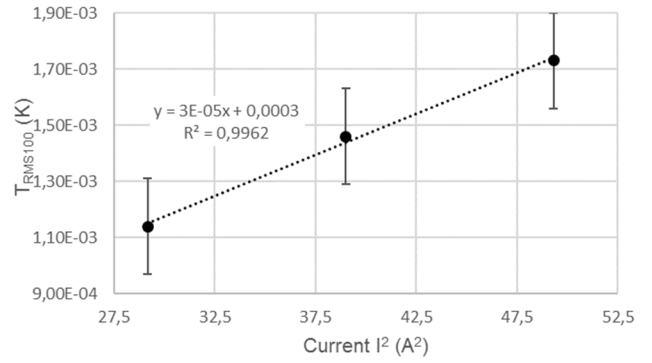
TABLE III
AVERAGE RMS VALUE OF THE OBTAINED HARMONICS OF
100 Hz OF THE TESTED SIGNALS

RMS current I (A)	5.4	6.24	7.02
T_{RMS100} (K)	$1.14\cdot10^{-3}$	$1.46\cdot10^{-3}$	$1.73\cdot10^{-3}$

TABLE IV
$T_{\mathrm{rms}100}$ VALUES FOR THE DARK AND LIGHT MEASUREMENTS

RMS current I (A)	dark, T_{RMS100} (K)	light, T_{RMS100} (K)	ΔT_{RMS100} (K)
5.4	$1.13\cdot10^{-3}$	$1.15\cdot10^{-3}$	$2\cdot10^{-5}$
6.24	$1.46\cdot10^{-3}$	$1.46\cdot10^{-3}$	0
7.02	$1.72\cdot10^{-3}$	$1.74\cdot10^{-3}$	$2\cdot10^{-5}$

In summary, the overall procedure of rms current measurement using the second-harmonic approach can be presented as below.

1) Registration of N thermal images $n = 16$ times for three values of current in a cable.
2) Extraction of temperature versus time $T(t)$ averaged in the chosen region of interest.
3) Filtering the signal $T(t)$ using bandpass (97–103 Hz) high-order FIR filter.
4) RMS value of temperature calculation.
5) Averaging rms value of temperature ($n = 16$ times).
6) Calibration finding the approximation formulae $T_{\mathrm{rms}100} = f(I_{\mathrm{rms}}^2)$ by using the linear or nonlinear regression.

B. Measurement in Dark and Light Environment

In addition, several attempts were made to register signals in 30 s, for three rms currents: 5.4, 6.24, and 7.02 A in conditions of total blackout (dark), and in the situation of natural light illuminating the steel wire. The signals were processed using the method mentioned earlier and the rms value of the temperature $T_{\mathrm{rms}100}$ for the 97–103-Hz spectral range was calculated (Table IV).

According to the results in Table IV, additional natural light has a negligible effect on the value of the 100-Hz component of temperature, which maximally differentiates the results by 20 μK of rms value. Increasing the current reduces the relative differences of dark and light signals.
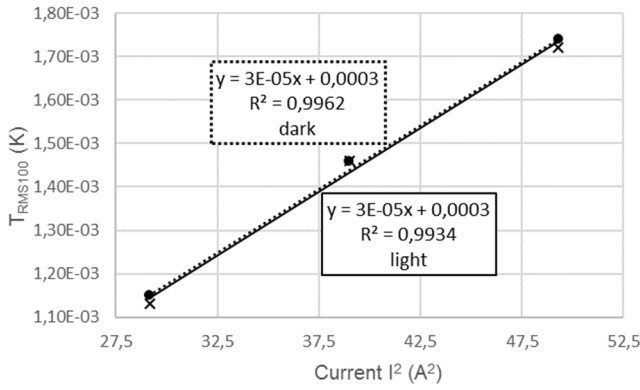
Fig. 12. Linear relations between rms value temperature in 97–103-Hz frequency versus the square of rms current for dark and light environments.

Natural light resulting from external atmospheric conditions, depending on the prevailing light intensity and spectral characteristics, should affect the temperature value recorded by an IR camera. Such effects are indeed noticeable but only for constant or low-frequency radiation within the absorption wavelength range of the used camera. Measuring the 100-Hz component of temperature filters dc and low-frequency parasitic signals significantly reduces their impact on power and current measurements. The proposed method is a kind of lock-in frequency-selective technique allowing reduction in the impact of external conditions. On the other hand, one must be aware that internal light generated by ac 50-Hz electrical current can dramatically change the measurement of temperature for the 100-Hz frequency. In the end, one can conclude that the proposed method is suitable for external conditions where there are sunlight reflections of high intensity from objects under test of low emissivity.

The linear nature of the rms values of the 100-Hz component of temperature regardless of the impact of natural light is shown in Fig. 12.

C. Measurement in Different Cooling Conditions

In order to check the effect of different environmental conditions, especially forced cooling, the tested wire was placed in the low-speed wind tunnel [Fig. 6(b)]. As before, the temperature signal was recorded within 30 s, 16 times, for the same current $I_{\mathrm{rms}} = 7.02$ A. Measurements were made for three preset wind speeds of 0.2, 0.42, and 0.66 m/s, which gives 16 measurement tests for each speed. The use of the tunnel allowed for a laminar and even air flow around the tested object, and air flow speed was measured using an anemometer [15]. The obtained recordings of temperature were subjected to the methods presented above in order to obtain the rms value of the 100-Hz component of temperature $T_{\mathrm{rms100.}}$ The mean temperature surplus of the tested wire above ambient ΔT_{mean} was measured for comparison (Table V).

Based on the data presented in Table V, it can definitely be confirmed that more intense air flow reduces the temperature ΔT_{mean} of the steel wire being tested. However, it has a negligible impact on the rms values of the 100-Hz harmonic of temperature signal. The difference between the individual values results only from measurement errors. The results

Air flow speed v(m/s)	0.2	0.42	0.66
ΔT_{mean} (K)	18.55	12.40	10.56
T_{RMS100} (K)	$1.66 \cdot 10^{-3}$	$1.69 \cdot 10^{-3}$	$1.70 \cdot 10^{-3}$

coincide with the thermal model presented in this research confirming that the presented new method of measuring the rms current value is valid, regardless of the cooling conditions of a wire, such as convection and radiation. This is one of the most important conclusions from a practical point of view, and makes it possible to recommend the presented method for use in varying environmental conditions.

VI. CONCLUSION

IR cameras that are often used in industry to record temperature changes allow monitoring additional parameters, for example, gas and liquid leakage as well as power or electrical current flowing in the conductor under voltage. The use of an appropriate method of analyses such as FFT or band-filtering allows correlating temperature changes and power rise in the tested objects. This article presents the quantitative application of available IR cameras to measure the rms value of electrical current. The calibration characteristic was determined and the linear relation of $T_{\mathrm{rms100}} = f(I_{\mathrm{rms}}^2)$ for $f \approx 100$ Hz was theoretically and experimentally confirmed.

The new method of noncontact current measurement using an IR camera was presented. It gives the possibility of recording temperature changes of 100 μK using the IR camera with NETD ≈ 18 mK. This measurement method was submitted to the Polish Patent Office [9]. In addition, the thermal model prepared and the measurements performed, confirm that cooling conditions have no effect on the measurement results.

The measurement of ac electrical current presented here does not depend on either natural light or external cooling conditions. This method can be easily extended for contact temperature measurements and nonsinusoidal electrical current with high value of the total harmonic distortion factors. After precise calibration, the proposed method can be used in industrial environments where parasitic phenomena have a significant impact on the measurement results.

The proposed method requires calibration prior to use in quantitative measurements. In some practical applications, e.g., for system maintenance, noncontact rms current can be measured periodically in the chosen place of the system to monitor changes and trends of the system parameters and finally, predict the failures. In such a case, the relative measurements can be made to increase the overall accuracy.

Extending current and temperature ranges of measurement in wires can result in nonlinearity of the characteristics $T_{\mathrm{rms100}} = f(I_{\mathrm{rms}}^2)$ caused by temperature dependent resistivity. The problem is beyond the main topic of the article and will be undertaken in the future research.

REFERENCES

[1] G. J. Anders, *Rating of Electric Power Cables in Unfavorable Thermal Environment*. New York, NY, USA: Wiley, 2005.

[2] W. Minkina, S. Dudzik, *Infrared Thermography: Errors and Uncertainties*. Hoboken, NJ, USA: Wiley, 2009.

[3] B. Więcek, G. De Mey, *Infrared Thermography, Basis and Applications*. Warszawa, Poland: PAK Publishing House, 2011.

[4] J. P. Brito Filho, "Heat transfer in bare and insulated electrical wires with linear temperature-dependent resistivity," *Appl. Thermal Eng.*, vol. 112, pp. 881–887, Feb. 2017.

[5] A. Sedaghat and F. De Leon, "Thermal analysis of power cables in free air: Evaluation and improvement of the IEC standard ampacity calculations," *IEEE Trans. Power Del.*, vol. 29, no. 5, pp. 2306–2314, Oct. 2014.

[6] I. Theodosoglou, V. Chatziathanasiou, A. Papagiannakis, B. Więcek, and G. De Mey, "Electrothermal analysis and temperature fluctuations' prediction of overhead power lines," *Int. J. Elect. Power Energy Syst.*, vol. 87, pp. 198–210, May 2017.

[7] B. Więcek, G. De Mey, V. Chatziathanasiou, A. Papagiannakis, and I. Theodosoglou, "Harmonic analysis of dynamic thermal problems in high voltage overhead transmission lines and buried cables," *Int. J. Electr. Power Energy Syst.*, vol. 58, pp. 199–205, Jun. 2014.

[8] B. Torzyk and B. Więcek, "Thermal modeling and RMS current measurement in electrical power lines using IR thermography," *Meas. Automat. Monit.*, vol. 64, pp. 53–56, Mar. 2018.

[9] B. Torzyk and B. Wiêcek, "A method of RMS current measurement especially in low and medium voltage power lines and cable," U.S. Patent 428 676, Jan. 2019.

[10] J. P. Amaro, R. Cortesao, J. Landeck, and F. J. T. E. Ferreira, "Harvested power wireless sensor network solution for disaggregated current estimation in large buildings," *IEEE Trans. Instrum. Meas.*, vol. 64, no. 7, pp. 1847–1857, Jul. 2015.

[11] J. C. Das and R. Mullikin, "Design and application of a low-ratio high-accuracy split-core core-balance current transformer," *IEEE Trans. Ind. Appl.*, vol. 46, no. 5, pp. 1856–1865, Sep. 2010.

[12] E. Hajipour, M. Vakilian, and M. Sanaye-Pasand, "Current-transformer saturation prevention using a controlled voltage-source compensator," *IEEE Trans. Power Del.*, vol. 32, no. 2, pp. 1039–1048, Apr. 2017.

[13] X. Xie, Z. Liu, C. Xu, and Y. Zhang, "A multiple sensors platform method for power line inspection based on a large unmanned helicopter," *Sensors*, vol. 17, no. 6, p. 1222, May 2017.

[14] J. Cho, J.-H. Kim, H.-J. Lee, J.-Y. Kim, I.-K. Song, and J.-H. Choi, "Development and improvement of an intelligent cable monitoring system for underground distribution networks using distributed temperature sensing," *Energies*, vol. 7, no. 2, pp. 1076–1094, Feb. 2014.

[15] *Electric Cables–Calculation of the Current Rating—Part 2-3: Thermal Resistance–Cables Installed in Ventilated Tunnels*, Standard IEC 60287-2-3:2017, 2017.

[16] *Electric Cables–Calculation of the Current Rating—Part 2-1: Thermal Resistance–Calculation of Thermal Resistance*, Standard IEC 60287-2-1:2015 RLV, 2015.

[17] *Calculating the Current-Temperature Relationship of Bare Overhead Conductor*, IEEE Standard 738, 2012.

[18] J. Arrillaga, N. R. Watson, *Power System Harmonics*, 2nd ed. Hoboken, NJ, USA: Wiley, 2003.

[19] L. Exizidis, F. Vallée, Z. De Grève, J. Lobry, and V. Chatziathanasiou, "Thermal behavior of power cables in offshore wind sites considering wind speed uncertainty," *Appl. Thermal Eng.*, vol. 91, pp. 471–478, Dec. 2015.

[20] S. Maximov, V. Venegas, J. L. Guardado, E. L. Moreno, and R. López, "Analysis of underground cable ampacity considering non-uniform soil temperature distributions," *Electr. Power Syst. Res.*, vol. 132, pp. 22–29, Mar. 2016.

[21] C. Holyk, H.-D. Liess, S. Grondel, H. Kanbach, and F. Loos, "Simulation and measurement of the steady-state temperature in multi-core cables," *Electr. Power Syst. Res.*, vol. 116, pp. 54–66, Nov. 2014.

[22] P. Chatzipanagiotou, "Dynamic thermal modelling and characterization of power lines," Ph.D. dissertation, Fac. Eng., School Elect. Comput. Eng., Aristotle Univ. Thessaloniki, Thessaloniki, Greece, 2018.

Błażej Torzyk received the B.Sc. degree in electronics and telecommunication and the M.Sc. degree in electrical engineering, specialization electric power engineering from the Lodz University of Technology, Łódź, Poland, in 2013 and 2015, respectively. He is currently working toward the Ph.D. degree at the Department of Electronic Circuits and Thermography, Lodz University of Technology.

His research interests lie in the field infrared (IR) thermography at power electronics systems and devices.

Bogusław Wiecek is the Head of the Electronic Circuit and Thermography Division, Institute of Electronics, Lodz University of Technology, where he has been working for more than 40 years. His scientific interests are heat transfer modeling, industrial and biomedical applications of infrared (IR) thermography, and IR system modeling and developments.

Mr. Więcek is responsible for organizing the largest conference on IR thermography in Central and Eastern Europe every two years–IR Thermography and Thermometry Conference.